

This work was partly supported by a Grant-in-Aid for Scientific Research from the Ministry of Education, Science and Culture, Japan (56430005) and by Itoh Science Foundation.

### References

*International Tables for X-ray Crystallography* (1974). Vol. IV, pp. 71–151. Birmingham: Kynoch Press.  
 JOHNSON, C. K. (1965). *ORTEP*. Report ORNL-3794. Oak Ridge National Laboratory, Tennessee.  
 KURIHARA, T., OHASHI, Y. & SASADA, Y. (1982). *Acta Cryst.* **B38**, 2484–2486.

KURIHARA, T., OHASHI, Y., SASADA, Y. & OHGO, Y. (1983). *Acta Cryst.* **B39**, 243–250.  
 KURIHARA, T., UCHIDA, A., OHASHI, Y., SASADA, Y. & OHGO, Y. (1984). *J. Am. Chem. Soc.* **106**. In the press.  
 MAIN, P., HULL, S. E., LESSINGER, L., GERMAIN, G., DECLERCQ, J.-P. & WOOLFSON, M. M. (1978). *MULTAN78. A System of Computer Programs for the Automatic Solution of Crystal Structures from X-ray Diffraction Data*. Univs. of York, England, and Louvain, Belgium.  
 OHASHI, Y. (1975). Unpublished version of an original program by T. ASHIDA.  
 OHASHI, Y. & SASADA, Y. (1977). *Bull. Chem. Soc. Jpn.*, **50**, 2863–2869.  
 OHGO, Y., TAKEUCHI, S., NATORI, Y., YOSHIMURA, J., OHASHI, Y. & SASADA, Y. (1981). *Bull. Chem. Soc. Jpn.*, **54**, 3095–3099.

*Acta Cryst.* (1984). **C40**, 1559–1562

## The Structure of $\text{PbI}_2$ -Pyridine Adducts. I. Lead(II) Iodide-Pyridine (2/4), *catena*-Di- $\mu$ -iodo-bis(pyridine)lead(II), $[\text{Pb}_2\text{I}_4(\text{C}_5\text{H}_5\text{N})_4]$

BY HIROSHI MIYAMAE, HIROSHI TORIYAMA, TOSHIKAZU ABE, GORO HIHARA AND MIHARU NAGATA

*Department of Chemistry, Faculty of Science, Josai University, Keyaki-dai, Sakado-shi, Saitama 350-02, Japan*

(Received 20 December 1983; accepted 10 May 1984)

**Abstract.**  $M_r = 1238.4$ , trigonal,  $P3_121$ ,  $a = 10.103$  (1),  $c = 24.584$  (3) Å,  $U = 2173.1$  (4) Å<sup>3</sup>,  $Z = 3$ ,  $D_m = 2.78$ ,  $D_x = 2.84$  Mg m<sup>-3</sup>, Mo  $K\alpha$ ,  $\lambda = 0.71069$  Å,  $\mu = 15.7$  mm<sup>-1</sup>,  $F(000) = 1632$ , room temperature, final  $R = 0.069$  for 1630 unique reflections. The two independent Pb atoms are on the twofold axes and are surrounded by four I and two N atoms. One Pb atom has regular octahedral coordination with the two pyridine molecules in *trans* positions, whereas the other exhibits very distorted octahedral coordination with the two pyridine molecules in *cis* positions. The two Pb atoms are alternately linked through the two bridging I atoms to form a helical chain along  $c$ .

**Introduction.** Lead(II) iodide ( $\text{PbI}_2$ ) reacts with some Lewis bases and its specific yellow color disappears. When the reaction products are allowed to stand in air they recover the original yellow color, indicating the loss of the Lewis bases. These facts seem to indicate that the Lewis bases intercalate between the layers of  $\text{PbI}_2$  to form 'intercalation compounds' (Koshkin, Mil'ner, Kukol', Zbrodskii, Dmitriev & Brintsev, 1976; Rybalka & Miloslavskii, 1976).

Independently, Wharf, Gramstad, Makhija & Onyszchuk (1976) discovered that pyridine (py), a typical Lewis base, forms two types of adducts with  $\text{PbI}_2$ :  $\text{PbI}_2(\text{py})_2$  and  $\text{PbI}_2(\text{py})$ . They proposed a linear chain structure for  $\text{PbI}_2(\text{py})_2$  on the basis of infrared spectra, where the two py molecules coordinate to the metal

atom in *trans* positions. However, they could not confirm it by single-crystal X-ray diffraction, because the compound was obtained as a fine powder.

We have succeeded in crystallizing the two adducts and determined the crystal structures in order to see whether intercalation occurs or not. This paper deals with one of the two products,  $\text{PbI}_2(\text{py})_2$ .

**Experimental.** Preparation as described by Wharf *et al.* (1976). The powder sealed was with ethanol in a branched glass tube, as shown in Fig. 1. An end of the branch containing the powder was kept at 333 K in a water bath and the other kept at ambient temperature (*ca* 293 K). After a week, crystals grew in the lower-temperature region. Crystal shows similar IR spectrum but much sharper X-ray powder diffraction pattern than those of original powder sample. Crystals

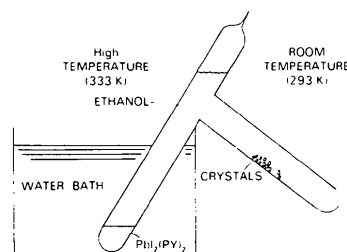


Fig. 1. Preparation of the crystals.

turned yellow in air on loss of py molecules.  $D_m$  by flotation. Colorless trigonal pyramidal crystal, 0.25 mm edge, 0.30 mm long, coated with epoxy resin to prevent deterioration, Rigaku AFC-5 diffractometer, graphite monochromator, unit-cell dimensions determined from least-squares fit of 44  $2\theta$  values ( $29 < 2\theta < 34^\circ$ ); intensities up to  $2\theta = 60^\circ$  [ $h \geq 0, k \geq 0 (h+k \geq 0), l \geq 0$ ],  $\theta$ - $2\theta$  scan mode, scan speed  $3^\circ \text{ min}^{-1}$  ( $\theta$ ), 4660 reflections measured, 1630 unique intensities ( $h$  0–13,  $k$  0–12,  $l$  0–34) with  $|F| \geq 3\sigma(|F|)$  considered observed and used for structure determination; intensities for four standard reflections measured after every 50 measurements varied by about  $\pm 1.5\%$  during data collection; correction for Lp factors; absorption correction assuming a simple trigonal pyramid improved  $R$  factor little; structure solved by heavy-atom and Fourier methods assuming space group  $P3_121$ , refined by block-diagonal least squares with anisotropic temperature factors for Pb and I atoms and isotropic for other atoms,  $\sum w|F_o| - |F_c|^2$  minimized,  $w = 1/\sigma^2(|F_o|)$ ;  $R = 0.069$ ,  $R_w = 0.066$ ,  $\Delta/\sigma$  max. = 0.3,  $\Delta\rho$  max. =  $2.2 \text{ e \AA}^{-3}$  in final  $\Delta F$  synthesis; real neutral-atom scattering factors from *International Tables for X-ray Crystallography* (1974); calculations carried out on FACOM M-150F and M-160F of this University with UNICS III (Sakurai & Kobayashi, 1978).

**Discussion.** A partial projection of the crystal structure along  $-b$  is shown in Fig. 2. Table 1 gives the positional parameters, Fig. 3 the numbering scheme.\* The py molecules are not simply incorporated in the crystal lattice of  $\text{PbI}_2$ , but coordinate to the Pb atoms, which form infinite  $[\text{PbI}_2]_n$  chains along  $c$ . However, this helical chain structure differs from the straight ones in  $\text{PbBr}_2(\text{Me}_2\text{SO})_2$  ( $\text{Me}_2\text{SO}$  = dimethyl sulfoxide; Baranyi, Onyszchuk, Le Page & Donnay, 1977) and in  $\text{PbI}_2(\text{Me}_2\text{SO})_2$  (Miyamae, Numahata & Nagata, 1980). The reason why this compound exhibits helical structure is not apparent but it is probably due to the presence of the inert lone pair of the Pb atom (see below). The molecular packing in the crystal is mainly realized through van der Waals interactions, since there are no inter-chain contacts shorter than 3.9 Å. Bond distances and angles around the Pb atoms are given in Table 2. The mean value of the Pb–I bond distance of 3.258 (3) Å is comparable to that of 3.22 Å in  $\text{PbI}_2$  (estimated from the data of Wyckoff, 1963). The entire geometry of the py molecules is quite normal.

The two Pb atoms on the twofold axis are both surrounded by four I and two N atoms. One of the Pb atoms is bonded by N atoms in *trans* positions [Pb(1)],

while the other is coordinated in *cis* positions [Pb(2)]. The structure consists of helical chains in which the *trans*- and *cis*-[ $\text{PbI}_4\text{py}_2$ ] units are alternately linked by sharing an I...I edge. Three pairs of *trans*- and *cis*-[ $\text{PbI}_4\text{py}_2$ ] moieties are in one period of the helix.

The Pb(1) atom is surrounded by six atoms in an almost regular octahedron, whereas the coordination octahedron around the Pb(2) atom is largely distorted. The N(2)–Pb(2)–N(2') [symmetry operation: (i)  $x - y, -y, \frac{2}{3} - z$ ] bond angle is about  $8.8^\circ$  smaller than  $90^\circ$ , but the py molecules avoid each other by rotating around the Pb–N bonds to keep the smallest C(10)···C(10') distance at 3.51 (4) Å.

Lawton & Kokotailo (1972) reported that in the case of  $[\text{Pb}\{(\text{i-C}_3\text{H}_7\text{O})_2\text{PS}_2\}_2]$  the bonds most remote from the 'stereochemically active lone pair', which originates from an inert  $6s^2$  pair, tend to be shorter than the other bonds and the lone pair occupies an equatorial position in an irregular pentagonal bipyramid. In the present case, the Pb(2), I(2), I(2'), N(2) and N(2') atoms are almost planar, the maximum deviation being 0.15 (2) Å

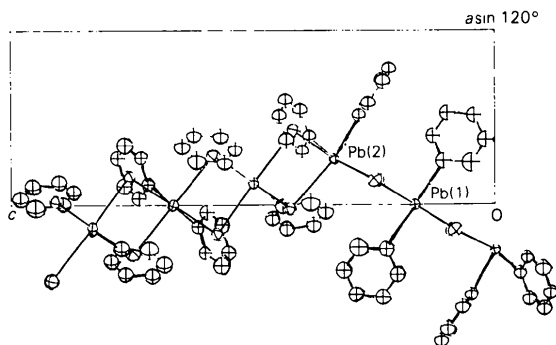


Fig. 2. ORTEP (Johnson, 1971) drawing of a partial projection of the unit cell along  $-b$ .

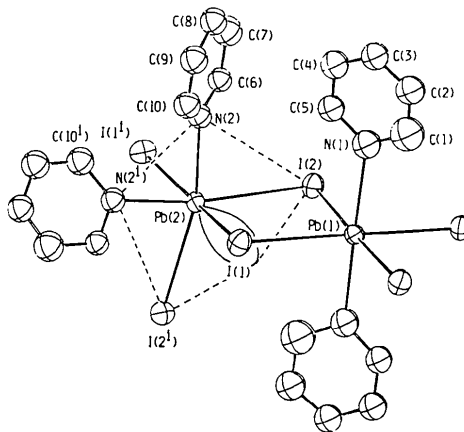


Fig. 3. A unit of the chain with atom numbering. The possible lone-pair site is shown by a lobe and dotted lines show the pentagonal plane of the *cis* form.

\* Lists of structure factors, anisotropic thermal parameters and bond distances and angles within the py molecules have been deposited with the British Library Lending Division as Supplementary Publication No. SUP 39481 (13 pp.). Copies may be obtained through The Executive Secretary, International Union of Crystallography, 5 Abbey Square, Chester CH1 2HU, England.

Table 1. *Positional* ( $\times 10^4$ ) *and isotropic thermal* ( $\text{\AA}^2$ ) *parameters*

	<i>x</i>	<i>y</i>	<i>z</i>	$B_{\text{eq}}/B_{\text{iso}}$
Pb(1)	0	-1265 (2)	1667	2.91 (4)†
Pb(2)	2612 (1)	0	3333	2.78 (5)†
I(1)	1429 (2)	-2820 (2)	2496 (1)	4.10 (8)†
I(2)	1419 (2)	1640 (2)	2423 (1)	3.67 (8)†
N(1)	2530 (26)	60 (28)	1066 (8)	4.3 (4)
N(2)	5132 (23)	1211 (26)	2815 (7)	3.6 (4)
C(1)	2439 (35)	-142 (38)	502 (10)	5.4 (6)
C(2)	3771 (34)	409 (34)	174 (11)	5.3 (7)
C(3)	5068 (36)	1060 (37)	454 (11)	5.2 (7)
C(4)	5240 (39)	1332 (42)	981 (12)	6.4 (8)
C(5)	3945 (35)	818 (35)	1296 (11)	5.4 (7)
C(6)	5792 (29)	2742 (31)	2679 (9)	3.5 (5)
C(7)	7101 (34)	3387 (35)	2340 (11)	4.8 (6)
C(8)	7788 (37)	2687 (40)	2200 (11)	5.6 (7)
C(9)	7109 (29)	1103 (29)	2352 (9)	3.4 (5)
C(10)	5775 (36)	372 (36)	2632 (10)	4.9 (6)

$$\dagger B_{\text{eq}} = \frac{4}{3} \sum_i \sum_j B_{ij} a_i^* a_j^* \mathbf{a}_i \cdot \mathbf{a}_j$$

Table 2. *Bond distances* ( $\text{\AA}$ ) *and angles* ( $^\circ$ ) *around the Pb atoms with e.s.d.'s in parentheses*

Symmetry operations: (i)  $-x, -x + y, \frac{1}{2} - z$ ; (ii)  $x - y, -y, \frac{2}{3} - z$

Pb(1)—I(1)	3.314 (3)	Pb(2)—I(1)	3.222 (2)
Pb(1)—I(2)	3.149 (2)	Pb(2)—I(2)	3.347 (2)
Pb(1)—N(1)	2.66 (2)	Pb(2)—N(2)	2.55 (2)
I(1)—Pb(1)—I(2)	88.60 (5)	I(1)—Pb(2)—I(2)	86.81 (6)
I(1)—Pb(1)—N(1)	92.5 (6)	I(1)—Pb(2)—N(2)	86.8 (5)
I(1)—Pb(1)—I(1 <sup>h</sup> )	92.39 (7)	I(1)—Pb(2)—I(2 <sup>h</sup> )	98.18 (5)
I(1)—Pb(1)—N(1 <sup>h</sup> )	89.3 (7)	I(2)—Pb(2)—N(2)	87.1 (6)
I(2)—Pb(1)—N(1)	89.1 (5)	I(2)—Pb(2)—I(2 <sup>h</sup> )	105.18 (7)
I(2)—Pb(1)—I(2)	90.45 (7)	N(2)—Pb—N(2 <sup>h</sup> )	81.2 (8)
Pb(1)—I(1)—Pb(2)	91.75 (7)	Pb(1)—I(2)—Pb(2)	92.42 (6)

for the N(2) atom. If the lone pair is assumed to be on this plane and almost behind the Pb(2)—I(1) bond in Fig. 3, as depicted by the lobe, the Pb(2) atom forms an irregular pentagonal bipyramid with the I(1) and I(1<sup>h</sup>) atoms in axial positions. This feature suggests that the inert lone pair is located behind two of the Pb(2)—N(2) bonds at the Pb(2) atom. Thus an increase in strength of the Pb—N bond causes more *s* character to be used in the bond for the Pb atom and more *p* character to be squeezed out into the lone pair in an equatorial position. Therefore an inert lone pair becomes a 'stereochemically active lone pair'. Consequently, the Pb—N bond distance in the *cis* form is shorter than that in the *trans* form.

The location of the lone pair deduced above can be supported by the axial I(1)—Pb(2)—I(1<sup>h</sup>) bond angle of  $171.8(1)^\circ$  directed slightly away from the I(2)—Pb(2)—I(2<sup>h</sup>) region. In contrast, the I(2)—Pb(2)—I(2<sup>h</sup>) bond angle of  $105.18(7)^\circ$  is quite small to accommodate the lone pair in this region. The Pb(2)—I(2) bond, which is *trans* to the Pb(2)—N(2) bond, is longer than the axial Pb(2)—I(1) bond by about  $0.13 \text{ \AA}$ . The latter bond length is almost equal to that in PbI<sub>2</sub>. The longer Pb(2)—I(2) bond distance might be a result of the electrostatic repulsion between the lone pair and the I(2) atom.

The *cis* form is largely distorted from a regular octahedron because of the lone pair squeezed out behind the Pb(2)—N(2) bonds. On the other hand, the lone pair in the *trans* form cannot aggregate and localize, since the two py molecules separate the lone pair in opposite directions. However, the Pb(1)—I(1) bond is longer than the Pb(1)—I(2) by about  $0.16 \text{ \AA}$ . The I(2) atom cannot bond firmly to the Pb(2) atom for the reason mentioned above, while the I(1) atom forms a normal bond with Pb(2). Assuming both I(1) and I(2) have equal covalence, the I(2) atom has to bond tightly to Pb(1). The alternating arrangement of the *cis* and *trans* forms may be attributed to the subtle balance between the Pb—N and Pb—I bond strengths and the lone-pair distribution.

When the compound releases the py molecules to recover the PbI<sub>2</sub> layer structure, the helical torsion of the [ $>\text{Pb}< \} ]_n$  chain of the structure should unravel, since the planar structure of PbI<sub>2</sub> has to be constructed from the non-spiral [ $>\text{Pb}< \} ]_n$  framework. In this connection, thermal analyses show that the powder sample prepared by direct reaction always decomposes in two steps, releasing a py molecule in each step, while a single-crystal sometimes shows a single-step decomposition.\* The IR spectra of both compounds are exactly similar, but the powder diffraction pattern of the direct reaction product shows similar but broad peaks to that of the single crystal. These facts indicate that the structures are slightly different, although both compounds comprise two types of Pb atoms which are coordinated by two py molecules in *cis* and *trans* positions alternately.

Part of the cost of this research was met by a Scientific Research Grant from the Ministry of Education, to which one of the authors' (HM) thanks are due.

\* When the differential thermal analysis was carried out with a slower heating rate, the vaporization of the py molecules was suppressed and the recombination to PbI<sub>2</sub> seems to be able to occur through a two-step decomposition.

## References

- BARANYI, A. D., ONYSZCHUK, M., LE PAGE, Y. & DONNAY, G. (1977). *Can. J. Chem.* **55**, 849–855.
- International Tables for X-ray Crystallography* (1974). Vol. IV. Birmingham: Kynoch Press.
- JOHNSON, C. K. (1971). *ORTEP II*. Report ORNL-3794 (revised). Oak Ridge National Laboratory, Tennessee.
- KOSHKIN, V. M., MIL'NER, A. P., KUKOL', V. V., ZABRODSKIL, YU. R., DMITRIEV, YU. N. & BRINTSEV, F. I. (1976). *Sov. Phys. Solid State*, **18**, 354–355.
- LAWTON, S. L. & KOKOTAILO, G. T. (1972). *Inorg. Chem.* **11**, 363–368.
- MIYAMAE, H., NUMAHATA, Y. & NAGATA, M. (1980). *Chem. Lett.* pp. 633–644.

RYBALKA, A. I. & MILOSLAVSKII, V. K. (1976). *Opt. Spectrosc.* **41**, 147–149.

SAKURAI, T. & KOBAYASHI, K. (1978). *Rikagaku Kenkyusho Hokoku (Rep. Inst. Phys. Chem. Res.)* **55**, 69–77. (In Japanese.)

WHARF, I., GRAMSTAD, T., MAKHJIA, R. & ONYSZCHUK, M. (1976). *Can. J. Chem.* **54**, 3430–3438.

WYCKOFF, R. W. G. (1963). *Crystal Structure*, Vol. 1, p. 269. New York: John Wiley.

*Acta Cryst.* (1984). **C40**, 1562–1563

## Structure of Dichlorobis(3,5-dimethylpyrazole-*N*<sup>2</sup>)zinc(II), [ZnCl<sub>2</sub>(C<sub>5</sub>H<sub>8</sub>N<sub>2</sub>)<sub>2</sub>]

BY E. BOUWMAN, W. L. DRIESSEN,\* R. A. G. DE GRAAFF AND J. REEDIJK

*Department of Chemistry, Gorlaeus Laboratories, State University Leiden, PO Box 9502, 2300 RA Leiden, The Netherlands*

(Received 21 March 1984; accepted 30 May 1984)

**Abstract.**  $M_r = 328.55$ , monoclinic,  $C2/c$ ,  $a = 15.013$  (3),  $b = 8.300$  (2),  $c = 23.988$  (7) Å,  $\beta = 95.85$  (2)°,  $V = 2973.6$  Å<sup>3</sup>,  $Z = 8$ ,  $D_x = 1.468$  g cm<sup>-3</sup>,  $\lambda(\text{Mo } K\alpha) = 0.71073$  Å,  $\mu = 20.27$  cm<sup>-1</sup>,  $F(000) = 1347.83$ ,  $T = 295$  K, final  $R = 0.033$  for 2430 significant reflexions. The Zn<sup>II</sup> ion is coordinated to the Cl<sup>-</sup> ions and the organic ligands in an irregular tetrahedral arrangement. The dimethylpyrazole molecules are planar. The least-squares planes of these molecules intersect at an angle of 84.9 (1)°. Hydrogen bonding between the N–H group of the pyrazole ring and the Cl<sup>-</sup> ions is relatively weak.

**Introduction.** 3,5-Dimethylpyrazole (abbreviated dmpz) forms a variety of complexes with transitional-metal ions. Metal-to-ligand bond formation occurs through the pyridine-type N atom. The chemical aspects of Zn(dmpz)<sub>2</sub>Cl<sub>2</sub> and related compounds have been discussed earlier (Guichelaar, van Hest & Reedijk, 1976). Although several X-ray structure analyses of pyrazole and pyrazole derivatives have been described, as for instance [Ni(pyrazole)<sub>6</sub>](BF<sub>4</sub>)<sub>2</sub> (ten Hoedt, Driessen & Verschoor, 1983) and [Co<sub>2</sub>F<sub>2</sub>(3,5-dimethylpyrazole)<sub>6</sub>](BF<sub>4</sub>)<sub>2</sub> (Jansen & van Koningsveld, 1976), structures of compounds with formula  $M(3,5\text{-dimethylpyrazole})_2X_2$  have not yet been reported. We have undertaken the X-ray structural analysis of Zn(dmpz)<sub>2</sub>Cl<sub>2</sub>, because of the stereochemical implications of the substituents at ring positions 3 and 5 and the influence of hydrogen-bond formation (N–H to anion) on the stoichiometry and structural details of this type of compound.

**Experimental.** Colourless prisms grown from ethanol at room temperature. Crystal approximately 0.6 × 0.3 × 0.25 mm. Enraf–Nonius CAD-4 four-circle diffractometer, graphite-monochromatized Mo  $K\alpha$ . Cell constants from setting angles of 24 reflexions. Corrections for Lorentz and polarization effects and absorption (transmission coefficients 0.87 to 1.11).  $\theta_{\text{max}} = 27.5^\circ$ ;  $h - 18$  to 18,  $k 0$  to 10,  $l 0$  to 30. Standard reflexions 242, 531 and  $\bar{1}39$ , intensity variation 4.1%. 7264 measured reflexions, 3634 independent,  $R_{\text{int}} = 0.017$ , 1186 unobserved with  $I < 2\sigma(I)$ .  $F$  used in LS refinement. Two out of three of the methyl H atoms placed 0.95 Å from the parent atoms, the others found in difference Fourier maps. Least-squares refinement of positional (H and non-H) and anisotropic (non-H) thermal parameters; positional parameters of hydrogen atoms coupled to parent atoms; fixed isotropic thermal factor of 4.0 Å<sup>2</sup> for the H atoms. Direct methods.  $S = 4.789$ ,  $w = 1/\sigma^2(F)$ ,  $R_w = 0.039$ .  $A_{\text{max}}/\sigma < 0.15$ . Max., min.  $\Delta\rho$  excursions in final difference synthesis 0.34,  $-0.35$  e Å<sup>-3</sup>. Scattering factors and anomalous-dispersion corrections from *International Tables for X-ray Crystallography* (1974). Leiden University computer (Amdahl V7B); programs written or modified by Mrs E. W. Rutten-Keulemans and R. A. G. de Graaff.

**Discussion.** Positional parameters and isotropic thermal parameters for the non-hydrogen atoms are listed in Table 1.† Relevant bond distances and angles

† Lists of structure factors, anisotropic thermal parameters and H-atom coordinates have been deposited with the British Library Lending Division as Supplementary Publication No. SUP 39516 (13 pp.). Copies may be obtained through The Executive Secretary, International Union of Crystallography, 5 Abbey Square, Chester CH1 2HU, England.

\* To whom correspondence should be addressed.